Application of two stage turbocharging systems on large engines

E. Codan, T. Huber
ABB Turbo Systems Ltd, Baden, Switzerland

ABSTRACT

The first applications of 2-stage turbocharging on large engines are already in operation (1), (2). The main drivers for the introduction of this technology are power density, engine efficiency and low emissions. In this paper some aspects and requirements of engine and turbocharging system design are discussed. Furthermore, some results of detailed studies for the different engine segments are presented. Engine size, operational envelope and performance requirements influence both the design parameters of the system and its development potential. Emissions represent a further challenge for large engines; the contributions of the turbocharging system are discussed.

NOMENCLATURE

p	Pressure (Pa, bar)
p_c	Compression pressure (bar)
p_{max}	Firing, maximum pressure (bar)
p_{me}	Brake mean effective pressure (bar)
p_{mi}	Indicated mean effective pressure (bar)
T, t	Temperature (K, °C)
V	Volume (m^3)
V_d	Displacement (m^3)
V_{298}	Reduced volume flow (m^3/s)
ε	Compression ratio
η	Efficiency
λ_C	Mass ratio of trapped to stoichiometric air
π	Pressure ratio

Subscripts

ac	Start of compression
ex	End of expansion
HD	Closed (high pressure) cycle
LWth	theoretical gas exchange
rec	charge air receiver
red	Reduced
TI	Turbine inlet

Abbreviations

BDC	Bottom dead centre
C	Compressor
CB	Constant boundary
CP	Constant pressure
EVO	Exhaust valve open
HP	High pressure
IVC	Inlet valve close
LP	Low pressure
T	Turbine
TDC	Top dead centre
VOL	Volume

1 THERMODYNAMIC ASPECTS OF THE TURBOCHARGED ENGINE

High pressure turbocharging in combination with the Miller process has recently been intensively investigated. Several studies have been performed by means of advanced simulation tools and confirmed by engine tests (3) (4) (5) (6). These studies show that there is substantial improvement potential for engine performance by applying 2-stage turbocharging in combination with Miller timing working at a boost pressure in the range of 8 bar and higher. Such a process relies on the reduction of the process temperatures

offered by the Miller process. This temperature reduction has a very positive effect on the engine's efficiency and its raw NO_x-emissions. At the same time, the high turbocharging efficiency achievable with 2-stage turbocharging allows the delivery of the required air pressure in an efficient way and additional power due to the improvement in gas exchange work.

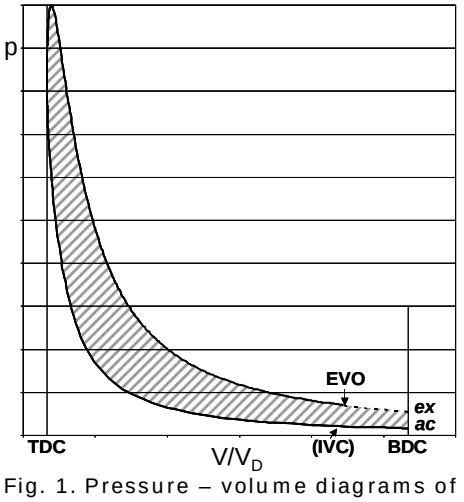

Fig. 1. Pressure – volume diagrams of the closed cycle

The above mentioned studies can be seen as a conventional approach to applying 2-stage turbocharging to further developed engines. Another approach is presented here, aimed at analysing and optimising the complete thermodynamic process of a 2-stage turbocharged engine. For this scope, the process is divided into three main parts: closed cycle; exhausting gas to the turbines; and charging air from the compressors. Additionally, some considerations are necessary regarding scavenging the combustion space and early closure of the inlet valve (Miller timing).

1.1 The closed cycle

The closed cycle is here defined as a process beginning and ending at BDC at the points start of compression (*ac)* and end of expansion (*ex)* (Fig. 1). These points are defined in the p–V diagram as extrapolations to BDC by means of an isentropic expansion of the respective points where the inlet valve closes (IVC) and the exhaust valve opens (EVO). In the case of Miller with IVC before BDC, the point *ac* is the effective start of compression.

Taking the closed cycle as the most important part of the process, one obviously must consider parameters like the compression ratio ε, firing pressure p_{max} and its ratio to compression pressure p_c. The latter plays a very important role in the trade-off between efficiency and NO_x-formation. Experience has shown that increasing p_{max}/p_c leads to better efficiency, albeit with higher NO_x emissions.

In a conventional cycle the points *ac* and *ex* are only connecting points to the gas exchange cycle. The point *ac* defines the available charge air per cycle; it is dictated by the required air/fuel ratio. The point *ex* depends on the engine energy balance; the pressure difference $p_{ex} - p_{ac}$ correlates directly with the difference between fuel energy and indicated work. With the introduction of the Miller cycle, the point *ac* acquires an additional degree of freedom. Theoretically the temperature t_{ac} could be reduced considerably, but there are limitations imposed by the increasing energetic losses of extreme Miller timing and by the issues of what we call "cold combustion" - it has been observed that below certain pressure and temperature values, especially at part load, diesel combustion assumes a knocking character with low efficiency and high NO_x-emissions. It has already been shown (3) that lowering the temperature at point *ac* reduces the temperature level of the whole closed cycle and this has a very positive impact on the cycle efficiency: at lower temperatures the specific heat of the charge air is reduced, i.e. less fuel energy is required for producing the same pressure increase in the cylinder. At the same time the lower combustion temperature reduces NO_x formation. The temperature at *ac* also has another consequence: a lower pressure p_{ac} is required for preserving the air/fuel ratio and the whole compression curve is lower, giving room

for increasing the ratio p_{max}/p_c, even at high λ and ε, without going beyond the design limit for firing pressure.

The curves in Fig. 2 show the evolution of the closed cycle efficiency over temperature t_{ac}. They have been calculated for a model engine in which IVC is varied under the following boundary conditions: the air/fuel ratio λ_C is maintained constant by varying charge air pressure p_{rec}, firing pressure has been kept constant by adjusting the start of injection, while the turbocharging efficiency of a 2-stage turbocharging system is approximately constant. The curves show some variability with different values of λ_C, but the general trend can be expressed as a slope of 1% of closed cycle efficiency improvement for 15 °C t_{ac} reduction. This result will be used in section 1.3 for evaluating the induction process.

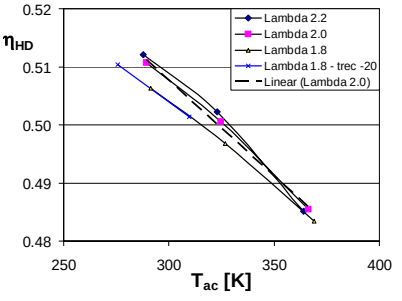

Fig. 2: Closed cycle efficiency over t_{ac}

1.2 The exhaust process

According to different engine cycle simulations for a highly turbocharged engine with Miller timing and an indicated mean effective pressure p_{mi} = 30 bar, values of p_{ex} = 11 bar and T_{ex} = 1000 K can be considered representative. For the sake of simplicity no scavenging is considered. The task is now to establish the maximum power that can be gained from the expansion of this exhaust gas. In this phase it is of secondary importance how this power is finally used. The work of the exhaust process has been idealised as shown in Fig. 3 (7). To make the following discussion more understandable, two curves have been plotted in the p-V diagram representing:

a) an isentropic expansion of the gas in the cylinder to ambient pressure starting from the point *ex* at BDC
b) a curve derived from a) assuming that the gas is collected in a manifold and expansion work outside the cylinder is dissipated.

With the help of the curves *a* and *b*, different exhaust processes, the ideal pulse and the ideal constant pressure process can be defined.

The ideal pulse process relies on using the blow-down energy. The gas expands to ambient pressure with the piston at BDC. This process would require putting the turbine in the position of the exhaust valve. The available energy is the sum of the areas 1 and 2.

The constant pressure process relies on filling a volume at an intermediate pressure p_{TI}. The blow-down energy is not converted into turbine expansion work and increases gas enthalpy to the turbine: the isentropic expansion in the diagram starts from the intersection of the p_{TI} line with curve *b*. The piston has to provide work during the exhaust stroke. The available energy for the turbine is given by the sum of the areas 2, 3 and 4, whereby area 4 is provided by the piston, i.e.

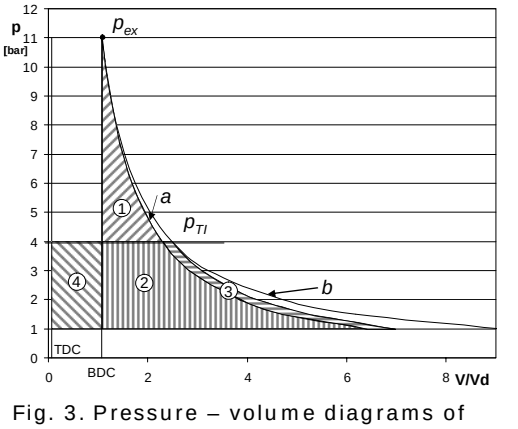

Fig. 3. Pressure – volume diagrams of the exhaust process

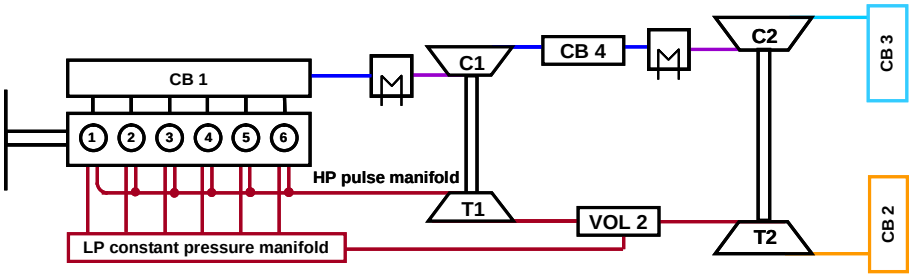

Fig. 4: Two-port pulse system

available engine power is reduced by this amount.

A further idea could be to use both systems in parallel. The availability of two turbine stages opens the theoretical possibility of realising an improved pulse process: a first exhaust valve opens during the blow-down phase and is connected via a pulse manifold to the high pressure (HP) turbine, working with energy corresponding to area 1. A second exhaust valve opens after the first one and is connected to an intermediate constant pressure manifold also receiving the gas from the HP turbine outlet. Gas from this manifold is admitted to the low pressure (LP) turbine which operates with the energy given by the areas 2 and 4. The topology of such a system is represented schematically in fig. 4.

A real pulse process is something between the two ideal cases. A fraction of the blow-down energy (area 1) can be utilised; the remaining fraction is converted into increased enthalpy for the steady flow expansion (area 3). Calling x the conversion rate of the blow-down energy, the available turbine energy is given by the sum of the areas 2 and 4 plus x times area 1 and (1-x) times area 3.

The evolution of the available power with the different ideal exhaust processes, pulse and constant pressure, starting with p_{ex} = 11 bar and t_{ex} = 1000 K, is represented versus the expansion ratio π_T (fig.5a). The turbine isentropic power with pulse (a) starts from a high value at expansion ratio 1 and increases in linear progression with the expansion ratio. The same line (c) for constant pressure starts from zero and reaches the line for pulse at the highest expansion ratio. The middle lines (b rsp. d) represent the net isentropic power, i.e. turbine power minus the piston power needed to expel the gas from the cylinder. The pulse line shows a slight negative slope; and the constant pressure curve shows again an increase from zero to the same final value. The line *e* is the net effective power of the exhaust process, applying constant overall turbine

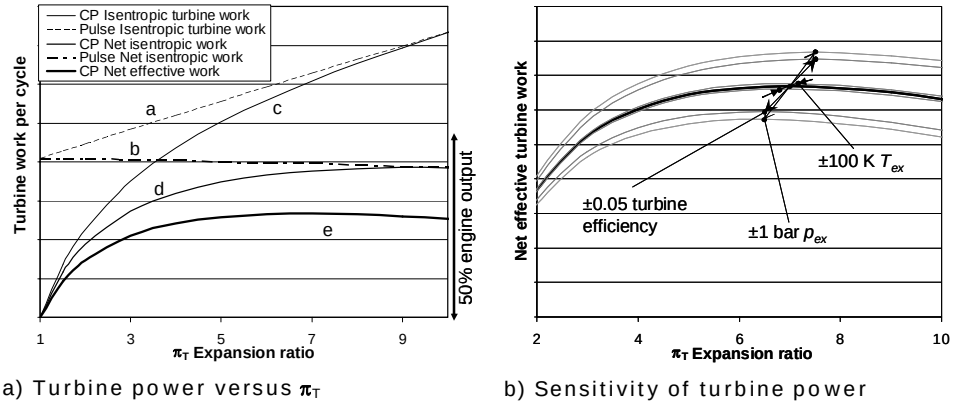

a) Turbine power versus π_T b) Sensitivity of turbine power

Fig. 5: Energy balance of the exhaust process.

efficiency. The curve now shows a very flat maximum at an expansion ratio of 7. The value of the curve is practically constant in the range from 6 to 8, which indicates the optimum range for matching the exhaust process of a very efficient engine.

A sensitivity analysis has been performed for the curve of effective power *e* with a constant pressure exhaust system (fig. 5b). The influences are listed as follows:

- ± 1% turbine efficiency ➔ ± 1.85% net turbine power
- ± 1% p_{ex} ➔ ± 1.6% net turbine power, ± 1% mass flow rate
- ± 1% T_{ex} ➔ ± 0.1% net turbine power, ∓ 1% mass flow rate

The curve of the effective power for the pulse system is missing since it is difficult to define an efficiency for the conversion of the blow-down energy. Simulations with different configurations have never produced a point above the line for constant pressure. This confirms that the assertion that (quasi) constant pressure systems are the most efficient full load ones for high pressure turbocharging is also valid for 2-stage turbocharging. On the other hand, the power of the pulse system at full load is only marginally lower and part load has not been studied, which leaves the door open for the use of pulse turbocharging for part load optimisation. Simulations with the system shown in Fig. 4 has shown inferior performance in comparison with a conventional pulse system, thus no further steps have been made for its realisation in practice.

1.3 The charging process

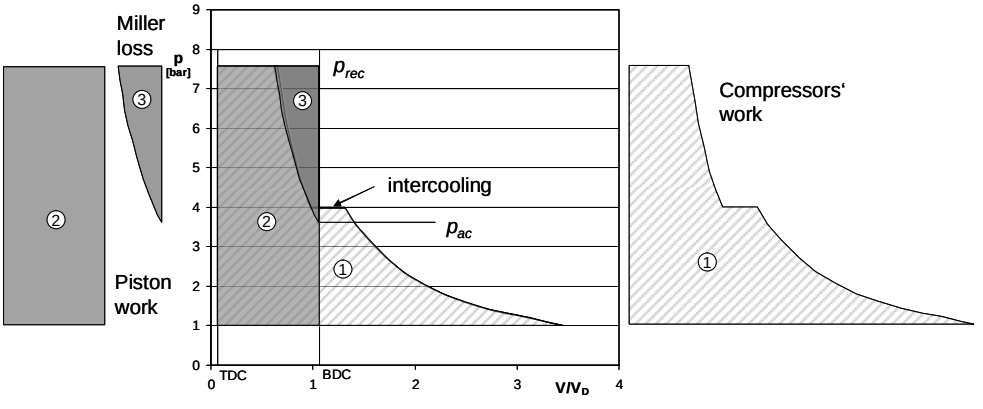

Fig. 6: p –V diagram of the charging process

After fixing the maximum power that can be extracted from the exhaust gas, the next step is to find out which is the most efficient way to use this power. The process is described in fig. 6. Area 1 represents the isentropic compression work for the air entering the cylinder. The intermediate step in the compression curve is the effect of the intercooler between the compressor stages. Area 2 is the work that would be gained from piston movement under receiver pressure. Area 3 is the loss of piston work due to the early IVC typical of Miller. Starting from this idealised process, in fig. 7 the different work contributions have been plotted versus the pressure ratio. The first curve (*a*) represents isentropic compressor work; the second (*b*) has been derived by applying suitable compressor maps and adapted intercooler temperatures according to water condensation. It can be noted that due to intercooling, the two curves are approximately parallel, i.e. the efficiency of the equivalent single stage compressor increases with the overall pressure ratio and the additional power required for a pressure increase is rather low in the upper range.

In order to calculate the net power required for the charge air, the gain in piston work (*c*) must still be taken into account (*d*), in addition to the gain in closed cycle work due to the reduction of t_{ac}. It can be noted that the curve *d* is very flat at its start. The plotted curve, obtained by means of an analytical approach, shows a flat minimum at a pressure ratio below 6. An approach by means of engine cycle simulation shows a monotone course for curve 4, i.e. the minimum occurs at pressure ratio 4, as defined by the λ_C requirement.

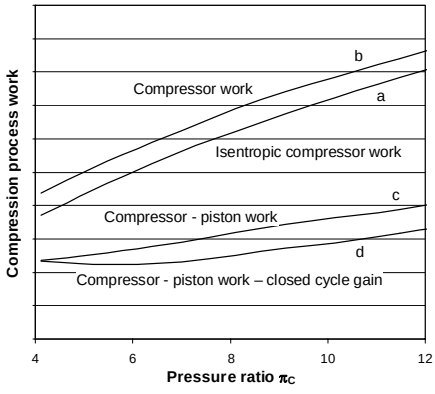

Fig. 7 Compressor work versus π_C

The conclusion of the results of the simulation, optimising both exhaust and charging processes would lead to an engine with an air pressure ratio of 4 (without Miller) and expansion ratio of 7. This high expansion ratio gives enough power to drive the compressors and, additionally, a turbocompound system producing roughly one third of the engine power. According to simulations, the efficiency of such a turbocompound engine shows 8% better values than the base engine with single stage turbocharging. Some drawbacks of this kind of engine would be higher NO_x-emissions, exhaust gas temperatures of around 630 °C and mechanical issues of power transmission.

1.4 The scavenging process

So far only the exhaust and charging processes for a non-scavenged engine have been considered. Consequently the exhaust gas temperatures are very high. Some scavenging is always present in reality on large engines. The scavenging process requires a positive pressure difference over the cylinder and leads to some efficiency reduction, but also has several advantages. A closer look into this process is thus necessary. Even without valve overlap there is some additional trapped air in the cylinder thanks to the positive pressure difference. This additional air is due to the fact that the residual gas in the clearance volume is compressed from p_{TI} to p_{rec}, leaving some volume free for fresh air, which could be considered as some kind of scavenging air. Starting from this mixture of residual gas and air, the influence of increasing valve overlap is analysed.

A set of simulations has been performed with constant pressures before and after the cylinder and with increasing valve overlap. The first point is simulated for reference without pressure difference over the cylinders; the other points have a fixed pressure difference of 2 bar, without considering turbocharging energy balance. A zero overlap is usually connected to high flow losses, due to the reduction in valve flow area before and after TDC. To avoid this, the points of maximum valve lift have been fixed and the overlap has been changed, with corresponding variation of the opening and closing ramps. The scavenging mass balance is shown in fig. 8a. After the step with zero overlap, caused by the reduction of pressure in the exhaust manifold, the mass of air introduced to the clearance volume is progressively increased. Up to about 40°CA the corresponding volume of residual gas is scavenged, but no significant mass of air should be present at the exhaust side. The global scavenging factor, defined as the ratio of the total air flow to the amount of trapped air is always 1, but with the overlap of 40°CA, almost 50% of the residual gas is already scavenged. Further increasing valve overlap produces better scavenging but the optimum range for efficiency seems to be between 50 and 60°CA. This is also shown by the curves in Fig. 8b, where engine and turbine power are slightly increased in parallel with the valve overlap. The compressor power curve has a comparable slope up to about 50°CA, after which compressor power

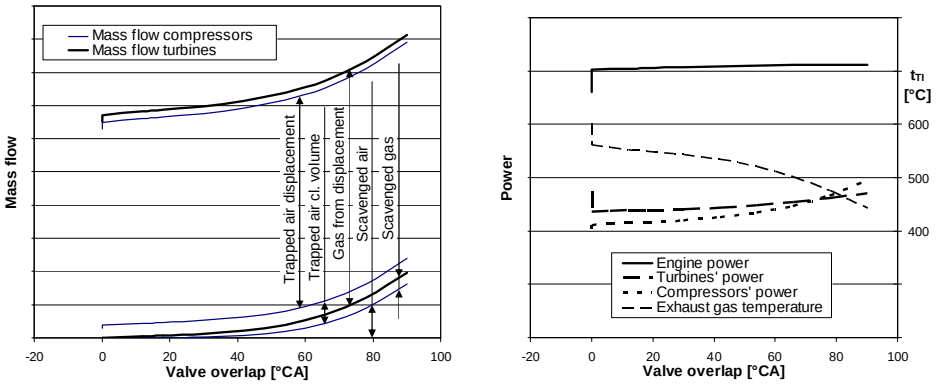

a) Mass balance

b) Power balance and t_{TI}

Fig. 8: Scavenging process

increases more steeply, impairing system efficiency. Under the chosen conditions the exhaust gas temperature reaches 500°C at an overlap of 66°CA. Going to even lower temperatures is not conducive to system efficiency.

1.5 The complete engine process

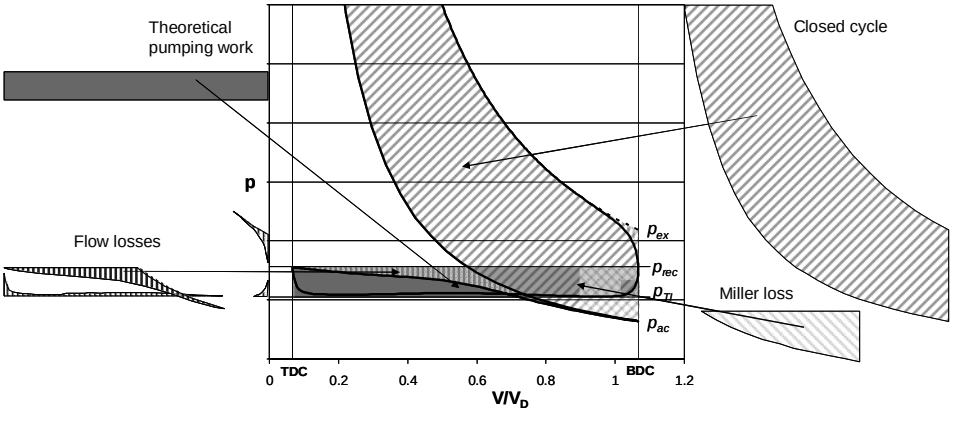

Fig. 9: Complete process analysis

So far the whole exercise has been conducted in such a way that the single processes have been analysed separately. In section 1.3 for example, considerations have been made with the degree of freedom that the turbine power must not necessarily be equal to compressor power. Without turbocompounding the air pressure ratio must be increased and the turbine expansion ratio reduced in comparison to the values given in 1.3. The minimum air pressure ratio of 4 would require a very low expansion ratio in the turbines, which would mean very bad utilisation of the exhaust gas energy. Increasing pressure ratio leads to a higher power requirement for the compressor, but better utilisation of the gas energy. This statement will be discussed further by looking into the complete engine process. Applying the previously presented method of analysing the single processes does not necessarily lead to an understanding of the complete process, due to the various and complex interactions between the single processes.

Instead of looking at the discharge, charging and scavenging processes, the overall process as characterised by the indicated mean effective pressure (p_{mi}) has been divided in four part processes (fig. 9):

- The closed cycle as defined in section 1.1 ($p_{mi,HD}$)
- Theoretical gas exchange, defined as pressure difference over the cylinders multiplied by displacement (p_{miLWth})
- The Miller loss, which gives the reduction of piston work during the induction process due to early IVC ($p_{mi,Miller}$)
- Flow losses through the valves; ($p_{mi,flow}$).

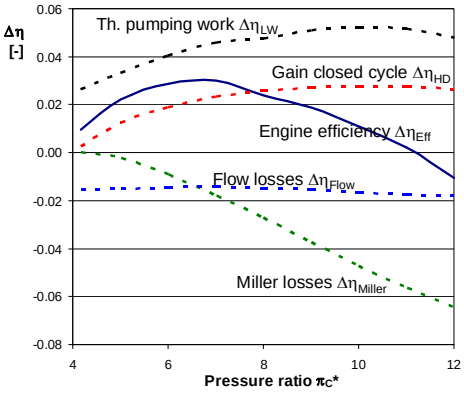

Fig. 10: Efficiency contributions

The flow losses through the valves are calculated from the difference between the work of the piston during the real gas exchange process and the theoretical work represented by p_{miLWth} minus $p_{mi,Miller}$.

These terms, expressed in the form of efficiency variations, are plotted in fig. 10 over pressure ratio for the same engine model as in the preceding sections. The efficiency values are obtained by multiplying the indicated mean pressure by the factor displacement, divided by heat input per cycle. This time the pressure ratio has been varied under following conditions:

- IVC has been adapted to for a constant air fuel ratio
- The start of injection has been adjusted for constant firing pressure
- Valve overlap has been adapted for constant exhaust gas temperature
- The temperatures of the intercooler and aftercooler have been adapted for a constant margin against water condensation
- Turbocharging efficiency remains approximately constant at a level of 75%.

Under these boundary conditions the curve for the possible gain in engine efficiency shows an optimum at pressure ratio of around 7. This is valid for the full load operation of an engine which is optimised with respect to engine efficiency. Additionally, this configuration gives a substantial reduction in the NOx emissions, while exhaust gas temperature remains moderate. Engine efficiency is about 6% (equal to 3 points efficiency in Fig. 10) better than the basic engine. Thus, the efficiency gain of this engine configuration is only 2% lower than that of the optimised turbocompound engine from section 1.3.

2 REQUIREMENTS ON THE TURBOCHARGING SYSTEM

Looking at the design of the 2-stage turbocharging system for 4-stroke engines under the aspect of fuel efficiency only, the target pressure ratio might be around 8. If we take into account the trade-off between efficiency and emissions, as well as the requirement to improve power density and altitude capability, a single figure compression ratio would not be the right solution. There will be a wide range of pressure ratios in the future; even with values above 10.

2.1 Pressure ratio distribution

Even if only total pressure ratio has been mentioned up to now, this still has to be broken down into single pressure ratios for each stage. It is well known that turbocharging efficiency defined according to (11) is a function of the pressure distribution between the low pressure stage $\pi_{C,LP}$ and the high pressure stage $\pi_{C,HP}$. The ratio $\pi_{C,LP}/\pi_{C,HP}$ which gives the maximum efficiency is a function of the intercooling temperature. It is convenient for reason of size to choose a ratio close to two. In this case the loss in global efficiency is marginal but the LP turbine area is smaller (fig. 11).

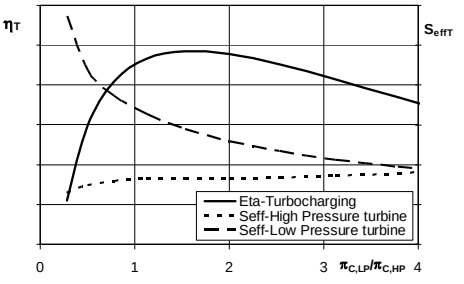

Fig. 11: Pressure repartition

By reducing engine load the pressure distribution is changed. The above mentioned diagram is valid for full load operation but the choice of the pressure distribution at full load also has an influence on its evolution over the engine load profile. It has been observed, that the pressure ratio of the HP turbocharger remains fairly constant in the upper load range. Within this range, the change of overall pressure ratio is determined by the low pressure stage only and the HP stage acts as a constant multiplier. According to simulations, for part load operation it is convenient to extend this constant multiplier range as far as possible. This can be achieved by increasing the ratio $\pi_{C,LP}/\pi_{C,HP}$.

An explanation for this behaviour can be found in Figure 12. For a constant overall pressure ratio this diagram shows the behaviour of the reduced turbine mass flow from both stages, plotted over the stage expansion ratio and the overall expansion ratio. The curves are similar to the flow characteristic of a nozzle. The reduced mass flow increases with the expansion ratio up to a maximum defined by the critical expansion ratio, and

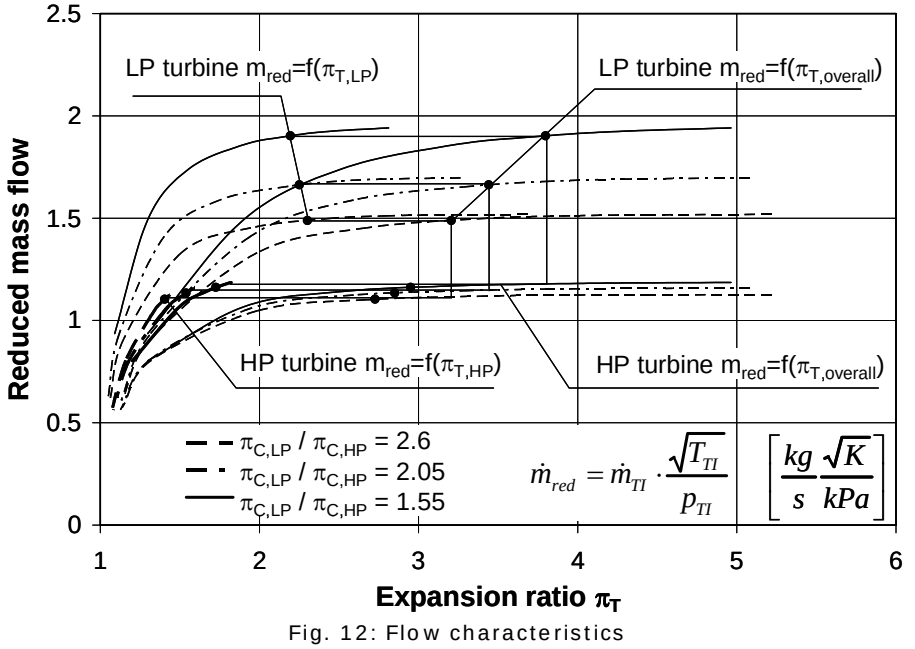

Fig. 12: Flow characteristics

then remains approximately constant. In this case the critical expansion ratio is defined with reference to 98% of the maximum flow. The critical expansion ratio for the whole system is about 2.8. When the LP stage has also reached its critical pressure ratio, the expansion ratio of the HP turbine can no longer be changed, even though it is well below its critical value. This condition occurs in the example of Fig. 12 at an expansion ratio of about 2.25 for the low pressure stage, which corresponds to an overall expansion ratio between 3 and 4, depending on pressure distribution at full load. The higher the ratio $\pi_{C,LP}/\pi_{C,HP}$, the earlier the low pressure stage attains its critical expansion ratio and the longer the $\pi_{C,HP}$ remains constant, leading to higher efficiency at part load.

2.2 Turbocharging efficiency

Turbocharging efficiency has always been important for achieving high pressure ratios at convenient exhaust gas temperatures. Two-stage turbocharging with intercooling ensures a substantial improvement, but the achievable efficiency is even more important than before. This is illustrated in fig. 13, where the achievable pressure difference over the cylinders is plotted versus the total pressure ratio for different turbocharging efficiencies and exhaust gas temperatures. This pressure difference, which is responsible for the theoretical gas exchange work, represents the most important contribution to engine efficiency (see fig. 10). The line of the Miller losses is plotted in the same diagram. An engine optimised for efficiency only should be matched well below the point where the curve of the Miller losses intersects the Δp curve. Taking the pressure loss over the cylinder and the Miller losses into account at the same time, it is logical to stay on the left side of the Miller loss curve. To achieve high pressure ratios it is thus mandatory to have high turbocharger efficiencies and exhaust gas temperatures as high as permissible.

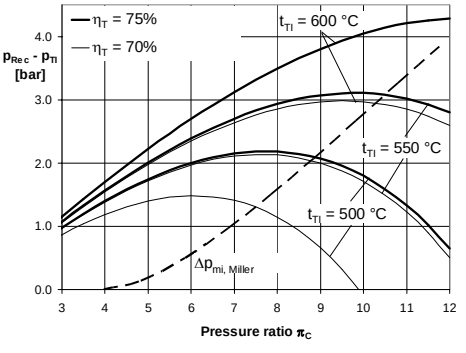

Fig. 13: Pressure difference over cylinder

2.3 Economic considerations

So far only the pressure ratio and efficiency of 2-stage turbocharging have been discussed. Flow capacity plays an important role in the physical dimensions of the 2-stage turbocharging system. The benefits of 2-stage turbocharging can be accessed in a profitable way by using components with high specific capacity. Fig. 14 shows the evolution of ABB/BBC compressor stages for a constant wheel diameter in terms of pressure ratio and flow capacity. It can be seen that the HP compressor stage is designed for a high capacity at moderate pressure ratio as well as ensuring a wide compressor map (fig. 15).

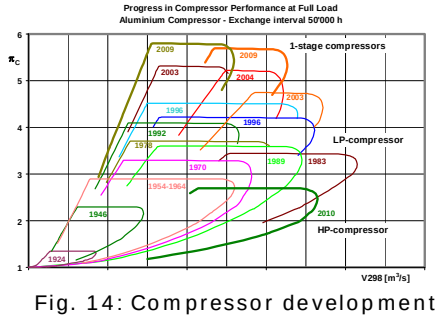

Fig. 14: Compressor development

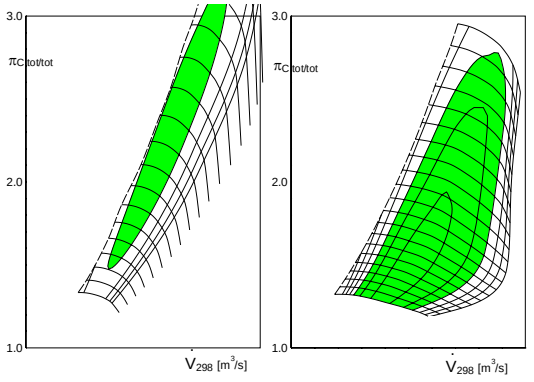

Fig. 15: HP Compressor map vs. standard compressor map (green areas: same efficiency)

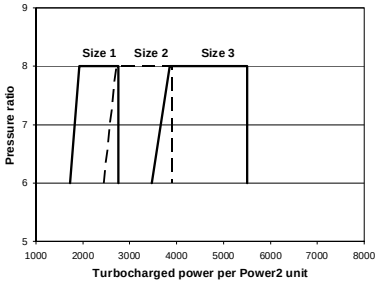

Fig. 16: Power 2 application ranges

2.4 Availability

First applications of the new ABB product known as Power2 two stage turbocharging have been documented in (1), (2). Two sizes of the first generation Power2 are available; a third size covering the power range from 2500 to 4000 kW will be launched according to market needs (fig. 16).

3 APPLICATION AND POTENTIAL OF POWER2 IN DIFFERENT ENGINE SEGMENTS

3.1 Engine models

Most simulations have been performed for a representative engine, and the results have been applied to different engine sizes. In order to achieve a better understanding of the potential of 2-stage turbocharging, an exhaustive series of simulations have been performed for different diesel engine models:

- Model A – Large medium-speed engine
- Model B – Small medium-speed engine
- Model C – High-speed engine

The results are summarized in the trade-off diagram in figure 17.

All engine models have been normalised to constant values of mean effective pressure, compression pressure and firing pressure. The reference points are valid for single stage turbocharging. The most important differences derive from the cylinder dimensions (bore and stroke) and rotational speed. As can be expected, fuel consumption increases from A to C due to size effects (combustion, heat losses, mechanical losses, turbocharging efficiency). The turbocharging systems and valve timings have been matched for air/fuel ratios and exhaust gas temperatures that are

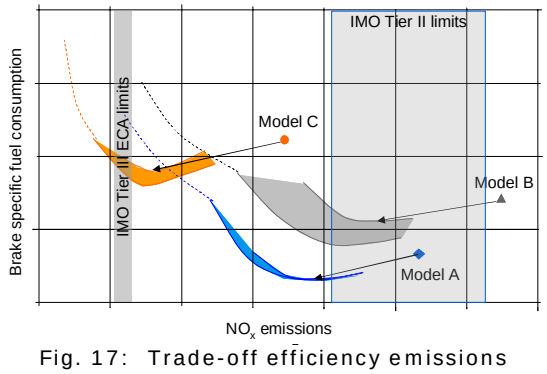

Fig. 17: Trade-off efficiency emissions

typical for medium-speed engines in HFO applications (A and B) and for high-speed engine running on distillate oil (C). Additional remarks:

- Model A. Engine and turbocharging efficiency are high with moderate scavenging.
- Model B. Due to the lower efficiency a higher scavenging ratio is required for to attain the same exhaust gas temperature as in A. This engine model has a larger stroke to bore ratio compared to the others. The comparatively lower speed has a positive effect on the efficiency but increases NOx-emissions.
- Model C. This model has a very small scavenging ratio and high exhaust gas temperatures. It has the highest specific fuel consumption and the lowest NOx-emissions.

The shaded areas represent the results obtained by applying 2-stage turbocharging and Miller timing under the following boundary conditions:

- Pressure ratios ranging from 6 to 12.5
- Constant air/fuel ratio and exhaust gas temperatures by adjusting Miller valve timing and valve overlap
- Constant compression and firing pressure by adjusting injection timing and compression ratio
- Variation in turbocharging efficiency.

For further evaluation a slightly higher exhaust gas temperature has also been considered for models A and B.
It can be seen that all the engines have a potential for a simultaneous reduction of specific fuel consumption and NOx-emissions. The difference between the 2 NOx-emission levels is approximately constant for all models, while model C can profit from the largest relative reduction.

Under the given boundary conditions, the pressure ratio related to highest efficiency is about 7 for the medium-speed engines, whereas for the high-speed engine it amounts to values above 8. This is a consequence of the higher exhaust gas temperature in accordance with Fig. 13.

The condition of constant compression and firing pressures keep the areas in a relatively narrow range. Increasing the ratio of firing pressure to compression pressure (not shown in the diagram) could lead to lower fuel consumption within the IMO Tier II NOx limits. Reducing the ratio by means of retarded injection (additional lines in fig. 17) could be used for achieving the lowest possible NOx-emissions. These lines give an indication of the possibility of reaching the low emission limits announced in IMO tier III and EPA Tier 4 by using only Miller timing and late injection. According to the applied simulation models, it seems that for the medium-speed engines and especially for engine B, the limits could only be approached in connection with a very high penalty in fuel consumption. With engine C the simulations show that very low emissions levels could be achieved. These considerations are limited to the nominal operation points at full engine load. At part load, the effect of Miller on emissions is substantially reduced, calling for additional emission reduction technologies. But the application of the proposed technology allows for substantial reductions in raw engine emissions and, consequently, reductions in the capacity required from the additional technologies.

Emission reduction technologies, typically selective catalytic reduction (SCR) and exhaust gas recirculation (EGR) are considered and have interactions with the turbocharging system. These interactions have been studied (8) and first experiments with the application are ongoing (9).

3.2 System flexibility.

It is well known that engines with extreme Miller timings require some kind of variability in terms of IVC. A solution is offered by ABB under the name VCM (Valve Control Management) (10). Medium-speed engines are typically used in constant speed applications or in a narrow speed range, e.g. baseload power generation and controllable (CPP) or fixed pitch propeller (FPP) operation. In all cases the operating points with maximum power and torque are met at nominal and maximum rated speeds. For these applications IVC variation is necessary for starting and loading the engine as well as for improving part load boosting for FPP applications.

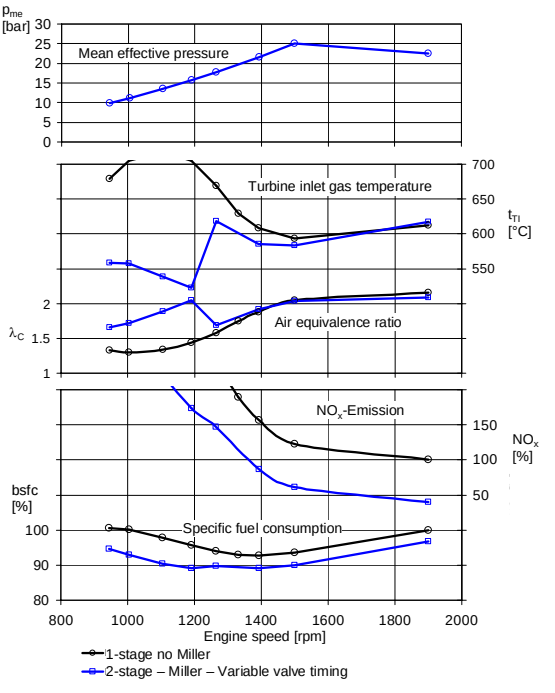

Fig. 18: Improved torque capacity with 2-stage turbocharging

High speed engines can cover a wider speed range and the point with maximum torque is not necessarily that with the highest speed. The potential of Power2 for this kind of application has been studied by means of simulations. As the engine operating curve an FPP curve with 10% torque rise from pme = 22.5 bar at 1900 rpm to pme = 25 bar at 1500 rpm has been considered (Fig. 18). With single stage turbocharging (boost pressure 4.7 bar) this operating curve is extremely challenging without additional control possibilities. At part load the maximum exhaust gas temperature is about 720°C with a very low air/fuel ratio (λ_C = 1.3). It can be noted that with Power2 (boost pressure 9.2 bar), Miller timing, and IVC variability, this very demanding curve can be operated with a much lower exhaust gas temperature and with a higher air/fuel ratio. In addition, fuel consumption is considerably reduced and transient behaviour can be expected to be much better.

CONCLUSIONS

A theoretical investigation on the turbocharged engine process has indicated that 2-stage turbocharging, extreme Miller timing, and variable inlet valve closure represents a very effective solution for engines with high power density. It is a proven measure for satisfying the requirements of high fuel efficiency in connection with low NOx emissions and high operational flexibility. With Power2 and VCM, ABB offers two of the core components for achieving these aims.

Power2 is the product name of ABB's 2-stage turbocharging concept, consisting at its minimum of an LP- and an HP-stage. The LP-stage is specifically designed for operation with high efficiency and high specific flow capacity. The HP-stage is specifically designed for operation at moderate pressure ratios, high volume flow and high absolute pressure with enhanced map width.

VCM (Valve Control Management) is offered as ABB's solution for variable valve timing. It is an electro-hydraulic system offering wide flexibility for control of valve timing as well as valve lift.

Additionally, the potential of this engine concept has been studied for different sizes of 4-stroke diesel engines. It has been shown that a range of engines can be positioned in a global trade-off diagram. Large medium-speed engine offer very good values of specific fuel consumption but high NOx-emissions whereas high-speed engines give higher fuel consumption and lower emissions. After a discussion of the specific characteristics of various engines, the feasibility of the concept for application on a high-speed engine featuring high torque requirements at variable speed has been evaluated.

REFERENCES

(1) Raikio, T., B. Hallbäck & A. Hjort, 2010, Design and first application of a 2-stage turbocharging system for a medium-speed diesel engine, 26th CIMAC World Congress in Bergen (N)
(2) Haidn, M., J. Klausner, J. Lang & Ch. Trapp, 2010, Zweistufige Hochdruck-Turboaufladung für Gasmotoren mit hohem Wirkungsgrad, 15. Aufladetechnische Konferenz, Dresden (D).
(3) Codan, E. & Mathey, Ch., 2007, Emissions – a new challenge for turbocharging, 25th CIMAC World Congress in Vienna, Austria
(4) Codan, E., Mathey, Ch. & Vögeli, S., 2009, Applications and Potentials of 2-stage Turbocharging, 14. Aufladetechnische Konferenz, Dresden (D).
(5) Codan, E., Mathey, Ch. & Rettig, A., 2010, 2-Stage Turbocharging – Flexibility for Engine Optimisation, 26th CIMAC World Congress in Bergen (N)
(6) Millo, F., Gianoglio, M. & Delneri, D., 2010, Combining dual stage turbocharging with extreme Miller timings to achieve NOx emissions reductions in marine diesel engines, 26th CIMAC World Congress in Bergen (N)
(7) Watson, N. & Janota, M.S., 1982, Turbocharging the internal combustion engine, MacMillan Press Ltd.
(8) Codan, E., S. Bernasconi, & H. Born, 2010, IMO III Emission Regulation: Impact on the Turbocharging System, 26th CIMAC World Congress in Bergen (N)
(9) Ruschmeyer, K, Rickert, C. & Schlemmer-Kelling, U., 2011, Potential des Caterpillar MaK 6 M32 C mit zweistufiger Abgasturboaufladung, 16. Aufladetechnische Konferenz, Dresden (D).
(10) Mathey, Ch., 2010, Variable Valve Timing – A necessity for future large diesel and gas engines, 26th CIMAC World Congress in Bergen (N)
(11) CIMAC, 2007, Turbocharging Efficiencies – Definitions and guidelines for measurement and calculation, Recommendation Nr. 27, Conseil International des Machines à Combustion, Frankfurt am Mein (D), (www.cimac.com)